CHAPTER 14

Optic nerve imaging

Larissa Camejo and Robert J Noecker

Glaucoma is an optic neuropathy with characteristic optic nerve appearance and visual field loss for which elevated intraocular pressure (IOP) is one of the main risk factors.[1] This characteristic optic nerve appearance results from structural glaucomatous changes which usually precede functional deterioration (visual field loss).[2,3] Therefore, improvement of the diagnostic methods of structural abnormality and change can result in earlier diagnosis of the disease.

Structural evaluations of the optic nerve head (ONH) and retina are key to the diagnosis and follow-up of glaucoma patients. Imaging tests complement slit-lamp biomicroscopy exam and stereo photos of ONHs. Ophthalmoscopy and even sequential stereo photos are dependent on the expertise and skills of the observer. High intra-observer and inter-observer variability has been demonstrated in several studies.[4,5] The goal is to diagnose the disease or its progression as early as possible, to increase the probability of preventing visual loss.[6,7]

There are three predominant imaging technologies currently in use for the diagnosis and evaluation of glaucoma in Europe and the U.S.[8] These devices are: confocal scanning laser ophthalmoscopy (CSLO) (the most common commercial application is known as Heidelberg retina tomography (HRT)); optical coherence tomography (OCT); and scanning laser polarimetry (SLP), whose commercial application is known as GDX. Scans of the ONH, retinal nerve fiber layer (RNFL) and of the macula have been studied for their relevance to glaucoma. Not all imaging technologies have the capability of imaging all three intraocular structures. The ONH can be scanned with HRT and OCT. The nerve fiber layer can be scanned with GDX and OCT, and the macula can be scanned with OCT. All these technologies work differently and have their own strengths and limitations as well as different measures of reliability. Full comprehension of all of these points will allow the clinician to accurately interpret the data obtained by each one of the imaging tests, as well as their correlation with one another. The ultimate goal is to improve the early diagnosis of glaucoma and detection of glaucomatous progression.

CONFOCAL SCANNING LASER OPHTHALMOSCOPY (CSLO)

HEIDELBERG RETINA TOMOGRAPHY (HRT)

Confocal scanning laser ophthalmoscopy is the imaging technology and HRT (Heidelberg Engineering, Heidelberg, Germany) is the major commercially available instrument that utilizes this imaging system to study the eye (Fig. 14-1). Heidelberg retina tomography has three generations: HRT, HRT II and HRT 3.

Confocal scanning laser ophthalmoscopy is capable of obtaining three-dimensional images of the optic disc by acquiring high-resolution images, both perpendicular to the optic axis (x- and y-axis) and along the optic axis (z-axis) (Fig. 14-2). It is based on the principle of spot illumination and spot detection. Conjugated pinholes are placed in front of the light source and light detector and allow only light originating from a determined focal plane to reach the detector. Sequential sections are obtained by moving the depth of the focal plane through the whole depth of the tissue being studied; in this case, the optic nerve. The focal plane depth is adjusted by shifting the confocal aperture or pinhole (Fig. 14-3).

Heidelberg retina tomography makes use of a 670 micron diode laser to perform rapid scanning of the fundus. Oscillating mirrors in the HRT device redirect the laser beam to the x- and y-axis, along a plane of focus that is perpendicular to the optic axis (z-axis). A bi-dimensional image (15 × 15 degrees) is obtained at each focal plane. As the device changes the focal plane, other bi-dimensional images of the optic nerve are obtained. Each one represents an optical section of the optic nerve. A total of 64 sections, each done with 1/16 mm of depth interval, are obtained and used to create a three-dimensional image of the optic nerve. These 64 sections are equivalent to a depth of 4 mm.

Each optical section is composed of 384 × 384 points compose each optical section. Each one of these points has an x (horizontal),

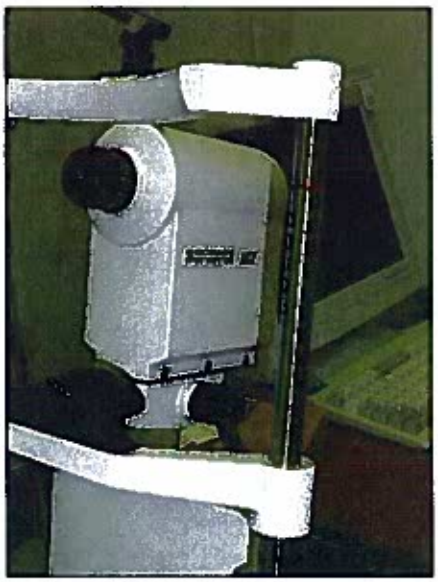

Fig. 14-1 Heidelberg retina tomography (HRT) II scanning laser ophthalmoscope.

y (vertical) and z (depth) value to locate it in space. The amount of light or 'reflectance' along the z-axis is measured at each scanned point, and the more intense the light is at a given point, the higher (closer to the surface) this is. In this way, the peak distribution of the reflected laser light intensity corresponds to the retinal/ONH surface. The peak intensity along the z-axis is assumed to correspond to the internal limiting membrane that overlies the retina and optic disc. A matrix of retinal height measurements is then created. The result is a topographical map of 384 × 384 height measurements of retinal and optic nerve surface topography. The light intensity measured at each one of the 384 points and used for the creation of the mean topography map is the result of an average of three scans which are automatically obtained by the newer generations of HRT. The transverse resolution is 10 microns and the axial resolution is 300 microns.

Once the image is taken, the operator delineates the optic nerve contour line over the reflectance or topography image. The operator places points at the external edge of the disc border and the machine draws a 'best-fit' ellipse linking these points together (Fig. 14-4). Heidelberg retina tomography proceeds to define the reference plane based on the disc contour drawn by the operator. The reference plane is located 50 microns posterior to the mean height along a 6° arc of the contour line at the temporal inferior sector. Structures above the reference plane and within the contour line are considered to be rim. Anything below the reference plane is considered cup (Fig. 14-5). Computation of stereometric parameters, classification of the eye and comparison to previous examinations are then done by the HRT. Classification of the eye is done with Moorefield's regression analysis or other discriminating method in HRT II, or with neural network analysis in HRT 3.

The latest software available, HRT3, can provide ONH stereometric analysis without manual delineation of the disc margin by the operator. After a three-dimensional model of the ONH is constructed, five optic nerve parameters are calculated and then

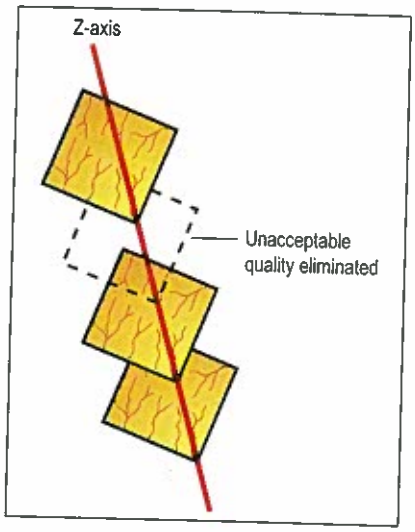

Fig. 14-2 Single images are obtained at different depths along the z-axis and aligned. Poor-quality images are eliminated in the process.

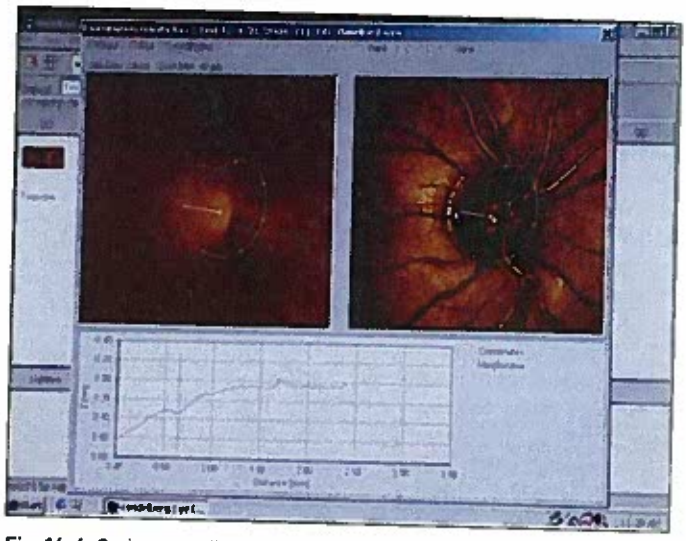

Fig. 14-4 Optic nerve disc delineation by operator.

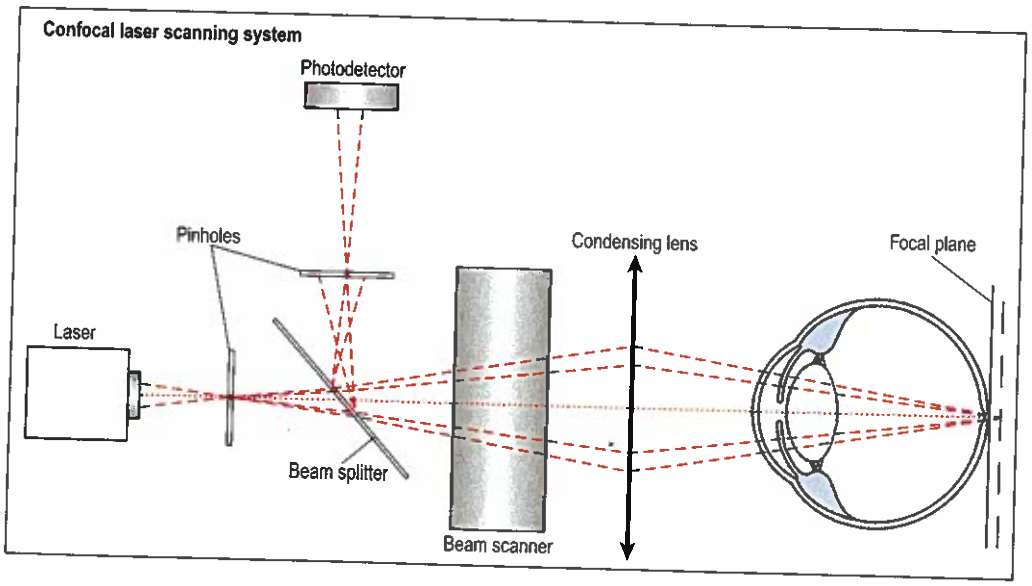

Fig. 14-3 Schematic diagram of a confocal scanning laser system used in HRT.
(Adapted from Fingeret M, Flanagan JG, Liebman JM: The esssential HRT primer. USA, Heidelberg Engineering, 2005.)[7]

analyzed with an artificial intelligence classifier, the relevance vector machine (RVM). From this analysis, a glaucoma probability score (GPS) is created.

Adjustments are made to the parameters to account for differences in age and disc size by both versions of HRT. However, HRT 3 is equipped with a larger and more diverse normative database than its predecessor. It currently includes large samples of three different ethnicities: Caucasian (>700), African descent (>200) and Indian or south-east Asian (>100). In comparison, the HRT II normative database includes 112 eyes, all from Caucasian subjects.

There are several printout formats currently available: initial report, follow-up report and 'OU report,' among others. Below, the different components of the HRT printout are discussed.

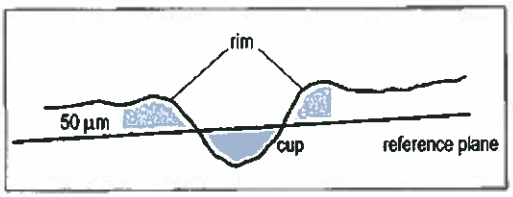

Fig. 14-5 Reference plane as calculated by HRT is based on disc contour delineation. The reference plane is defined as 50 microns posterior to the mean height along 6° of the contour line at the temporal inferior sector. Structures above the reference plane and within the contour line are considered as rim. Structures below the reference plane are considered cup.

Components of the HRT report

1. *Patient data:* name, sex, date of birth, patient ID, and date of exam are provided here (Figs 14-6 and 14-7).

2. *Topography image:* located on the left upper corner of the printout. It is a false-color image. More superficial areas appear darker and deeper areas appear of a lighter color. Additional colors are added to the map: red indicates the cup (area below the reference plane) and green and blue indicate neuroretinal rim tissue (above the reference plane). Blue indicates sloping rim.

3. *Reflectance image:* located in the right upper corner of the unilateral report or below the topography image on the 'OU report.' It is also a false-color image and is similar to a photograph with the brighter areas representing highest reflectance, like the cup. The reflectance image is overlaid with Moorfields analysis.

4. *Retinal surface height variation graph:* this appears once the disc contour is drawn and accepted. It is the graphical representation of the retinal height along the contour line and of the thickness of the nerve fiber layer. A green line represents the retinal height and a red line represents the reference plane. The graph depicts, from left to right: the thicknesses of the temporal (T); temporal-superior (TS); nasal-superior (NS); nasal (N); nasal-inferior (NI); temporal-inferior (TI); and temporal (T) sectors. Because the thickness of the normal retina is irregular, the contour line will appear as what is known as the 'double-hump.' The hills or 'humps' correspond to the superior and inferior nerve fiber layer, which are normally thicker than the rest of the areas.

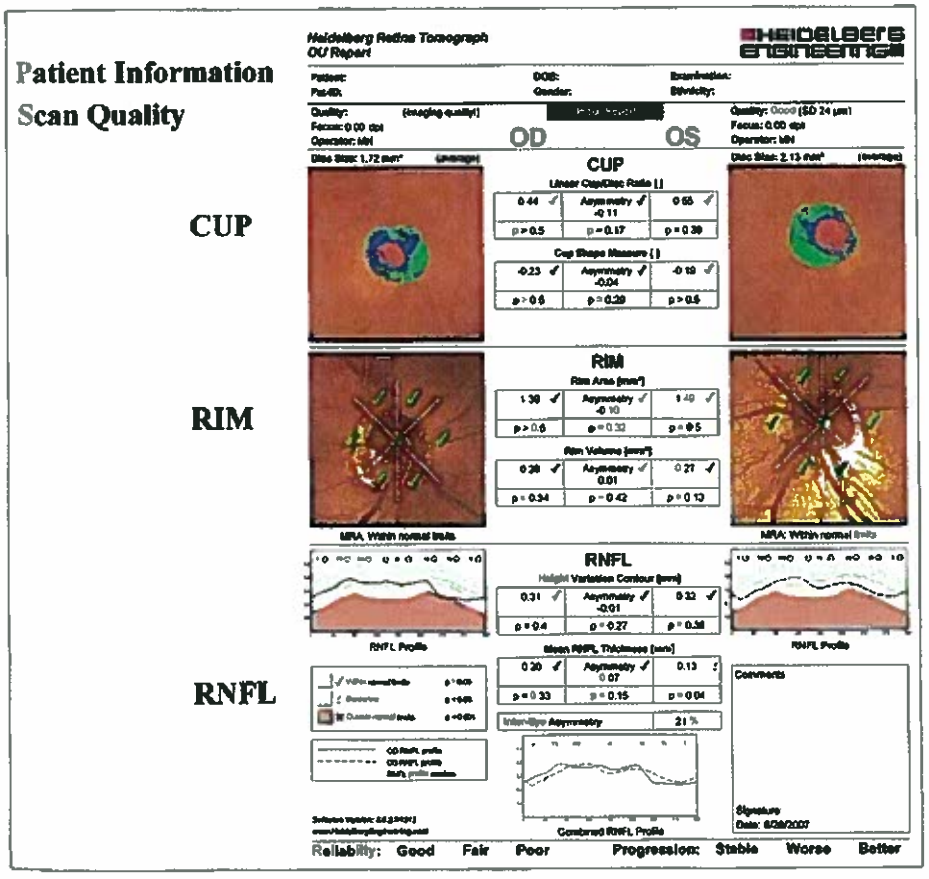

Fig. 14-6 HRT 3 baseline printout. After patient information, a Quality score is provided with classification for quick quality assessment. Scores below 30 represent good quality images. The cup section represents the disc topography. The CUP parameters shown in this row are cup/disc (C/D) area ratio and cup shape measure. The RIM section represents reflectance data with overlay of mean rim area (MRA) classification. The middle column shows rim parameters: rim area and rim volume. The last section contains the RNFL profile graph. It displays the height values at the optic disc margin going around the optic disc from the temporal side, to superior, nasal, inferior, and back to temporal (TSNIT). The green shaded area gives the normal range for that particular age, optic disc size, and ethnicity. Height measures that fall into the yellow zone are borderline, and those that fall into the red zone indicate abnormal values.

Patient Information

Scan Information

Topography

Horizontal (H) cross-section. Vertical (V) cross-section is in between topography and reflectance images. Retinal surface height graph to right.

Stereometric paramters. Moorfields regression graph to right.

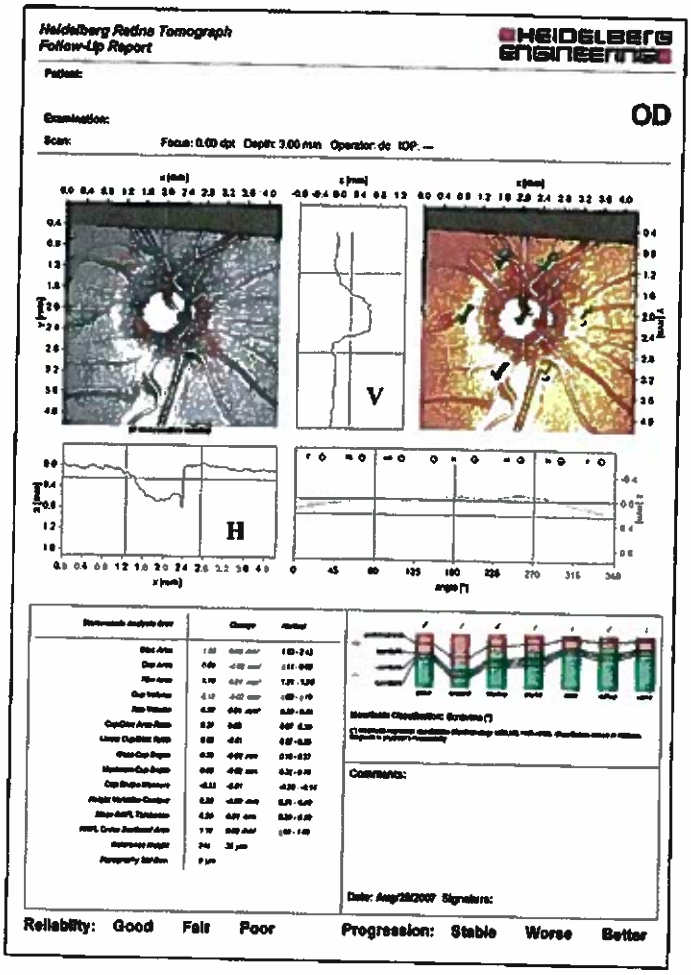

Fig. 14-7 HRT II baseline printout.

5. *Vertical and horizontal interactive analysis:* these are the optic nerve retinal surface height horizontal and vertical cross-sections. A smooth trace as opposed to a 'jagged' trace represents a better quality scan. Observation of the trace can provide information of the disc steepness, presence of sloping, etc.

6. *Stereometric analysis:* HRT II provides a list of 14 nerve parameters. They are: disc, cup and rim area, cup and rim volume, cup/disc area ratio, linear cup/disc ratio, mean cup depth, maximum cup depth, cup shape measure, height variation contour, mean retinal nerve fiber layer (RNFL) thickness, RNFL cross-sectional area and reference height. To the right of the stereometric parameters, a column specifies ± one standard deviation from the mean of the normative database for each of the parameters. HRT 3 only provides values for 6 stereometric parameters in the 'OU printout.' These are: cup/disc area ratio, cup shape measure, rim area and volume, height variation contour and mean RNFL thickness. Each value is designated as within normal limits, borderline or outside normal limits after comparing to the normative database.

7. *Moorfields regression analysis (MRA):* the MRA is based on a normative database of 112 Caucasian subjects with refractive error <6D and disc size within the range of 1.2–2.8 mm. A predicted rim area/disc area line was obtained after plotting the ratio values among these subjects. Such a predicted line represented the value obtained in 50% of the normal subjects studied. Further classification limits were obtained. In this way, if the rim area of any segment (global assessment or any of the 6 sectors) is below the 99.9% prediction interval, the nerve is classified as outside normal limits (red x). In other words, 99.9 % of 'normals' have a higher rim area/disc area value than that of the nerve being classified as outside normal limits (ONL). If the rim area falls between the 95% and 99.9% prediction lines, it is classified as borderline (yellow checkmark). Rim areas that fall above the 95% prediction level are classified as within normal limits (green checkmark). The Moorfields analysis graph is shown in the printout, indicating the predicted intervals on which the nerve classification is based. Seven different columns representing all sectors are shown and classified as within normal limits (WNL), borderline (BL) or ONL. Green color represents the rim and red represents the cup. Moorfields classification is also shown over the reflectance image as a green checkmark, yellow exclamation point, or a red 'x.' The Moorfields classification of the nerve is written at the bottom of the graph. Moorfields regression analysis classifies discs based on the worst classified sector.

8. *Glaucoma probability score (GPS):* new software included in the HRT 3 generation allows calculation of the GPS. It is based on the construction of a three-dimensional model of the ONL and peripapillary RNFL by using five parameters: cup size, cup depth, rim steepness, and horizontal and vertical RNFL. The complete three-dimensional model is then subjected to analysis by an artificial

intelligence classifier, the relevance vector machine (RVM), that compares it to a predetermined normal and glaucoma model and then derives the probability of glaucoma for the scanned eye:

- Probability ≤ 28% – within normal limits (WNL)
- Probability > 28% – borderline (BL)
- Probability ≥ 64% – outside normal limits (ONL).

Evaluating scan quality

Only data extracted from a scan of good quality is valuable. Therefore, it is of the utmost importance to know how to identify a poor quality scan. Good quality indicators are even luminance and sharp borders of the topography and reflectance images, as well as good centration of the disc. The standard deviation (SD) is a measurement of variability of the same pixel values among three different scans. The average light intensity for each point is what is used for the RNFL height measurement. The manufacturer has suggested not analyzing scans with a SD value greater than 40. It is important to point out that SD should not be the only parameter to use when assessing quality. A poor quality scan can still have a low SD value if there is small or no variability among the three scans.

The manufacturer's classification of scans by SD values is:

- <10: excellent
- 11–20: very good
- 21–30: good
- 31–40: acceptable
- 41–50: poor
- >50: very poor.

Looking at cross-sections can also help determine the degree of noise in the obtained images. The contour cross-sectional trace should be soft and not 'jagged.'

Strengths and limitations

Heidelberg retina tomography allows for rapid and simple operation and for three-dimensional representation of the optic nerve without the need for pupil dilation. Heidelberg retina tomography was used in one of the largest glaucoma clinical trials, the Ocular Hypertensive Treatment Study (OHTS), and therefore a large amount of data is available.[10,11]

Limitations of the HRT include the use of a reference plane that depends on the contour line drawn by the operator. Measurements might be affected by the blood vessels. The nasal border of the nerve can be difficult to identify given that blood vessels can appear crowded in this area and obscure the disc's edge. *Confocal scanning laser ophthalmoscopy is appropriate for scanning the ONH but not the macula or RNFL.*

Substantial inter-observer variability exists among HRT parameters, depending on the placement of the contour line. The most dependent parameters were rim volume and disk area and the least dependent were mean height contour and cup shape in one study.[12]

Higher rim measurements obtained from HRT optic nerve analysis compared to planimetric evaluation of disc photos are thought to be in part a result of blood vessel inclusion as part of the disc.[13,14] These limitations are secondary to potential errors in the delineation of the nerve done by the operator. The GPS analysis bypasses this problem. Early studies regarding the reliability of GPS analysis and its comparison with conventional HRT-MRA analysis are available.[15–17]

Heidelberg retina tomography's capability of discrimination between normal and glaucomatous patients has been tested in the past, and parameters were compared to search for the best discriminating parameters. Among the best parameters were cup shape measure, rim area and cup volume.[18,19] Nevertheless, combining parameters can render the strongest discrimination between groups. Different methods have been designed to analyze the data. Mikelberg's discriminating analysis and MRA are part of HRT software. Moorfields regression analysis can discriminate glaucomatous nerves from normals with 84.3% sensitivity and 96.3% specificity.[20,21] Still, the HRT will occasionally call a severely damaged optic nerve normal or a normal optic nerve abnormal.

Heidelberg retina tomography tends to overestimate rim area in small optic nerves and to underestimate rim area in large nerves. So on either extreme of disc size range, care should be taken when analyzing these scans.

New developments

The latest generation is HRT 3. HRT 3 includes the same MRA classification as HRT II, but it is based on a larger, more diverse normative database. It also assigns a GPS to the optic nerve disc. The GPS is based on three optic disc parameters and two RNFL parameters. A three-dimensional optic nerve is constructed and compared to preconstructed models of normal and glaucomatous nerves and a GPS is assigned to the nerve being tested. This analysis is independent of optic nerve contour delineation.

Testing from the patient's perspective

The patient's experience is similar to that of having a slit lamp exam and definitely more comfortable than having a fundus photo taken. The luminance of the diode laser is 100 times lower than the luminance of a digital fundus flash camera. The diode laser used in HRT is safe to the eye. A typical imaging session can be completed in less than 7 seconds.

OPTICAL COHERENCE TOMOGRAPHY (OCT)

Optical coherence tomography (Carl Zeiss Meditec, Inc., Jena, Germany), developed in 1991,[22,23] is an imaging technology that performs high-resolution, cross-sectional imaging of the ONH, RNFL and macula. It measures the intensity and echo time delay of back-scattered and back-reflected light from the scanned tissues (Fig. 14-8). Optical coherence tomography is analogous to ultrasound B-mode imaging, the difference being that the former uses light and the latter uses sound. It is based on the principle of low coherence interferometry and the ability to differentiate retina layers depending on the different time delay of their reflections.

A super luminescent 820 or 850 nm diode laser beam is the light source directed to a partially reflecting mirror that splits the light into two beams: one is directed towards a mirror placed at a known distance (reference mirror) and the other is directed towards the eye, from where it will reflect back. This back-reflected light will consist of multiple echoes, with information about the distance and thickness of the different intraocular tissues. The back-reflected light from the eye is combined with the back-reflected light from the reference mirror and coherent light is compared. Interference is produced when two light pulses coincide. The reference mirror is then moved so that the time delay of the reference light pulse can change accordingly and therefore other intraocular structures can be measured (Figs 14-9 and 14-10). The laser beam is panned throughout the tissue and a series of scans are obtained in the manner explained above, until a two-dimensional map is created based on the interference signals detected. The map is color coded in a way that white and red represent areas with high reflectivity and

blue and black represent areas with low reflectivity. High reflectivity layers include the nerve fiber layer, retinal pigment epithelium (RPE) and choriocapillaris. Low reflectivity layers or tissues include the photoreceptor layer, choroids and pockets of fluid.

Unlike other machines, OCT has the ability to scan three distinctive ocular structures: the peripapillary RNFL, the optic nerve, and the macula (Fig. 14-11). Optical coherence tomography has the best axial resolution of all the imaging devices presented here. OCT 3 has a resolution of 8–10 microns and the latest Ultra-high resolution has an impressive axial resolution of 3–4 microns. On the other hand, transverse resolution is limited secondary to the limited number of sampling points obtained by OCT. Different

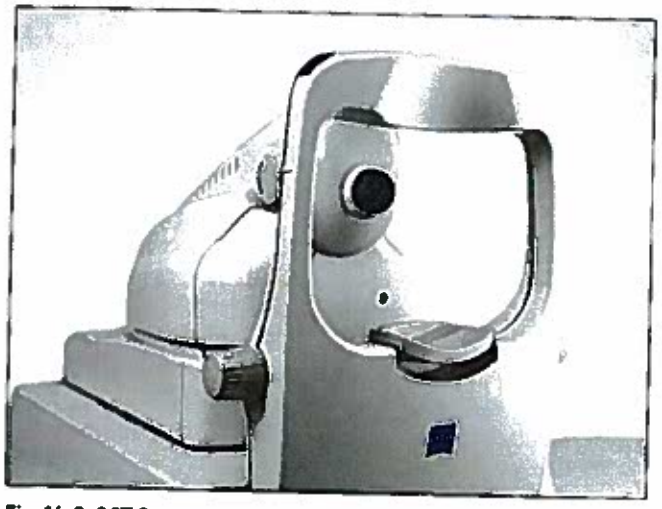

Fig. 14-8 OCT Stratus.
(Courtesy of Zeiss Meditec, Inc., Jena, Germany.)

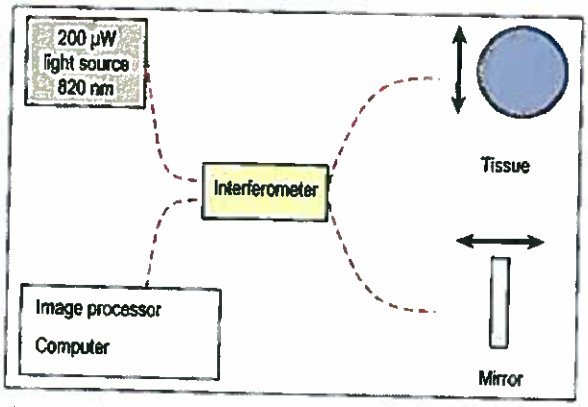

Fig. 14-10 This is a diagragm of the fiber-optic interferometer in the OCT imaging system. Low-coherence superluminescent diode is coupled into an optical fiber and directed into an optical fiber coupler (beam splitter), where one fiber forms the measurement path and the other the reference path. The fiber in the measurement path is connected to a clinical imaging device such as a fundus camera of a slit-lamp biomicroscope.
(Adapted from Schuman JS, Puliafito CA, Fujimoto JG: Everyday OCT: a handbook for clinicians and technicians, NJ, USA, Slack Inc., 2006.)[24]

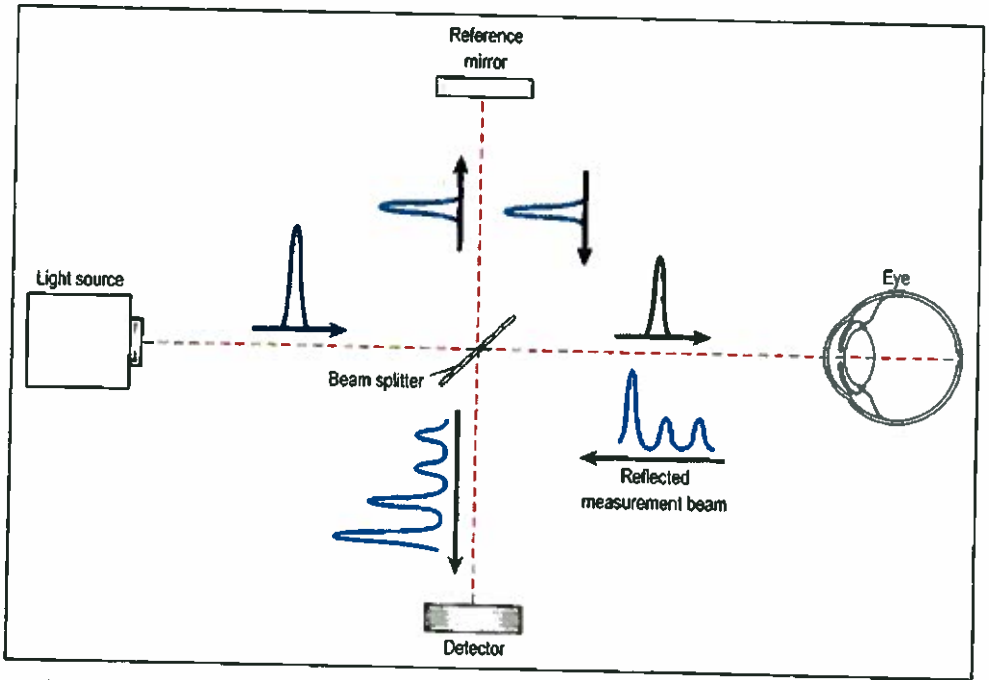

Fig. 14-9 Low-coherence interferometry system used in OCT. A superluminescent 850 nm diode laser beam is directed to a partially reflecting mirror that splits the light into two beams: one is directed towards a mirror placed at a known distance (reference mirror) and the other is directed towards the eye, from where it will reflect back. This back-reflected light will provide information about the distance and thickness of the different intraocular tissues. The back-reflected light from the eye is combined with the back-reflected light from the reference mirror and coherent light is compared. Interference is produced when two light pulses coincide. The reference mirror is then moved so that the time delay of the reference light pulse can change accordingly and therefore other intraocular structures be measured.
(Adapted from Schuman JS, Puliafito CA, Fujimoto JG: Everyday OCT: a handbook for clinicians and technicians, NJ, USA, Slack Inc., 2006.)[24]

generations of OCT exist: OCT 1, OCT 2, OCT 3 or Stratus OCT, and OCT Spectral (Fig. 14-12); Newer technologies include spectral domain and fourier domain OCT; these show higher resolution than previous OCT versions.*

DIFFERENT SCANNING MODALITIES

Peripapillary scan

This consists of a 3.4 mm circular scan that is used to measure the thickness of the RNFL. A RNFL curve is obtained by 'opening up' the circular scan. The RNFL curve starts with the temporal quadrant and continues clockwise in the right eye and counterclockwise in the left eye. The RNFL thickness values are provided for the four quadrants (temporal, superior, nasal, and inferior) and for 12 clock hours. Tested optic nerves are classified as within normal limits, borderline or outside normal limits, after comparing their RNFL thickness values to those of the normative database. The outcomes are also color coded. Green means within normal limits, yellow, borderline, and red, outside normal limits. Classification of RNFL thickness is assigned to all sectors and clock hours of the nerve but an average RNFL is also established.

Macular scan

This consists of six linear scans in a spoke pattern configuration. The linear scans are spaced 30° apart.

The length of the linear scans can be 3 mm or 6 mm. The longer 6 mm scan is more commonly used. The 'fast macular scan' utilizes 128 A-scans for each radial linear scan. It is possible to choose 256 and even 512 A-scans. Variability of measurements might decrease by using more sampling points (more A-scans), but the time of the test might increase as well, which could ultimately cause errors in image registration by jeopardizing the patient's ability to maintain fixation. A color-coded (blue represents thinner retina and yellow-green-red represents thicker retina) macular thickness map and a map with quantitative measurements in nine sectors is derived from the macular scan. The map depicted is a cross-sectional map along one of the six radial scans (a small map will show which axis is being analyzed).

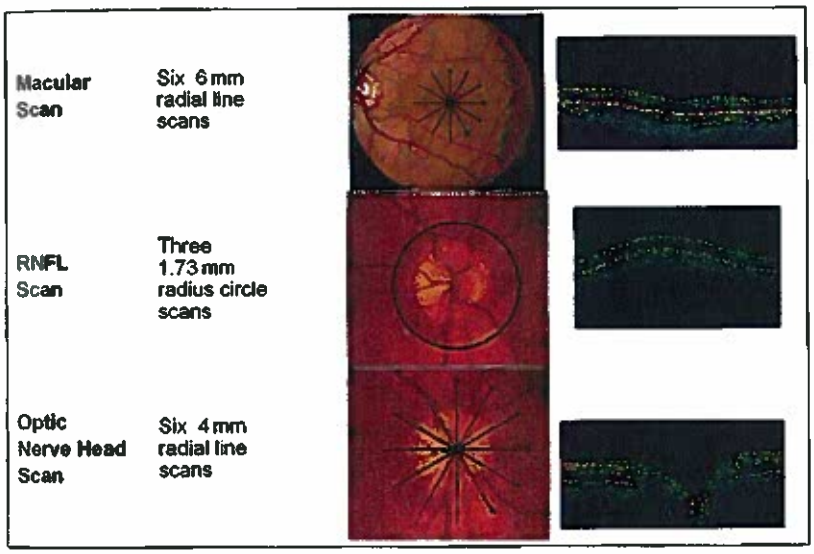

Fig. 14-11 Different OCT scanning modalities. **(A)** Linear scan used in macular scan, **(B)** fast macular scan; **(C)** circular scan of RNFL; **(D)** linear scan used in ONH scan. (Courtesy of Zeiss-Meditec, Inc., Jena, Germany.)

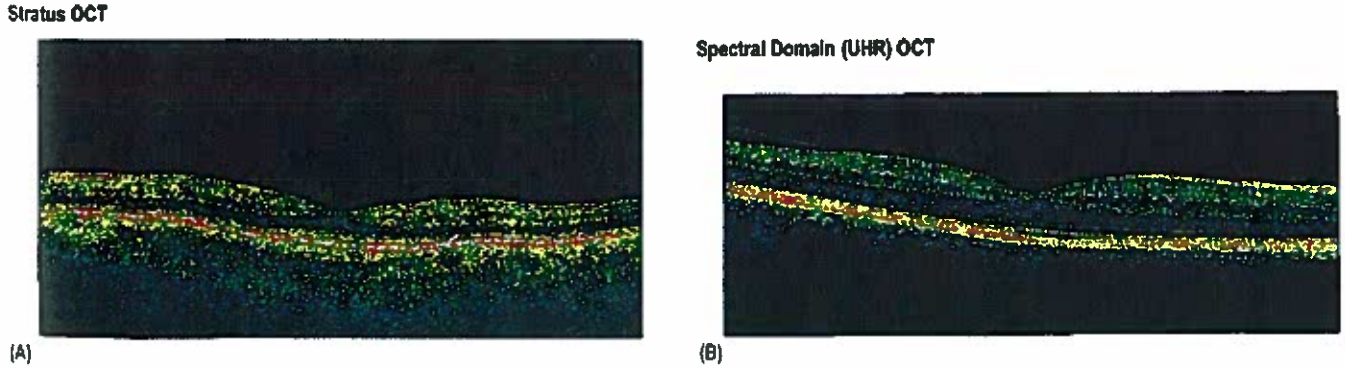

Fig. 14-12 **(A)** Stratus OCT image of macula area. **(B)** Spectral domain OCT image of macular area. Note higher resolution and clearer delineation of retinal layers compared to Stratus OCT.
(Courtesy of Zeiss-Meditec, Inc., Jena, Germany.)

*Several new devices from different manufacturers were appearing on the market as this book goes to press. The superiority of these higher resolution devices for clinical purposes remains to be demonstrated.

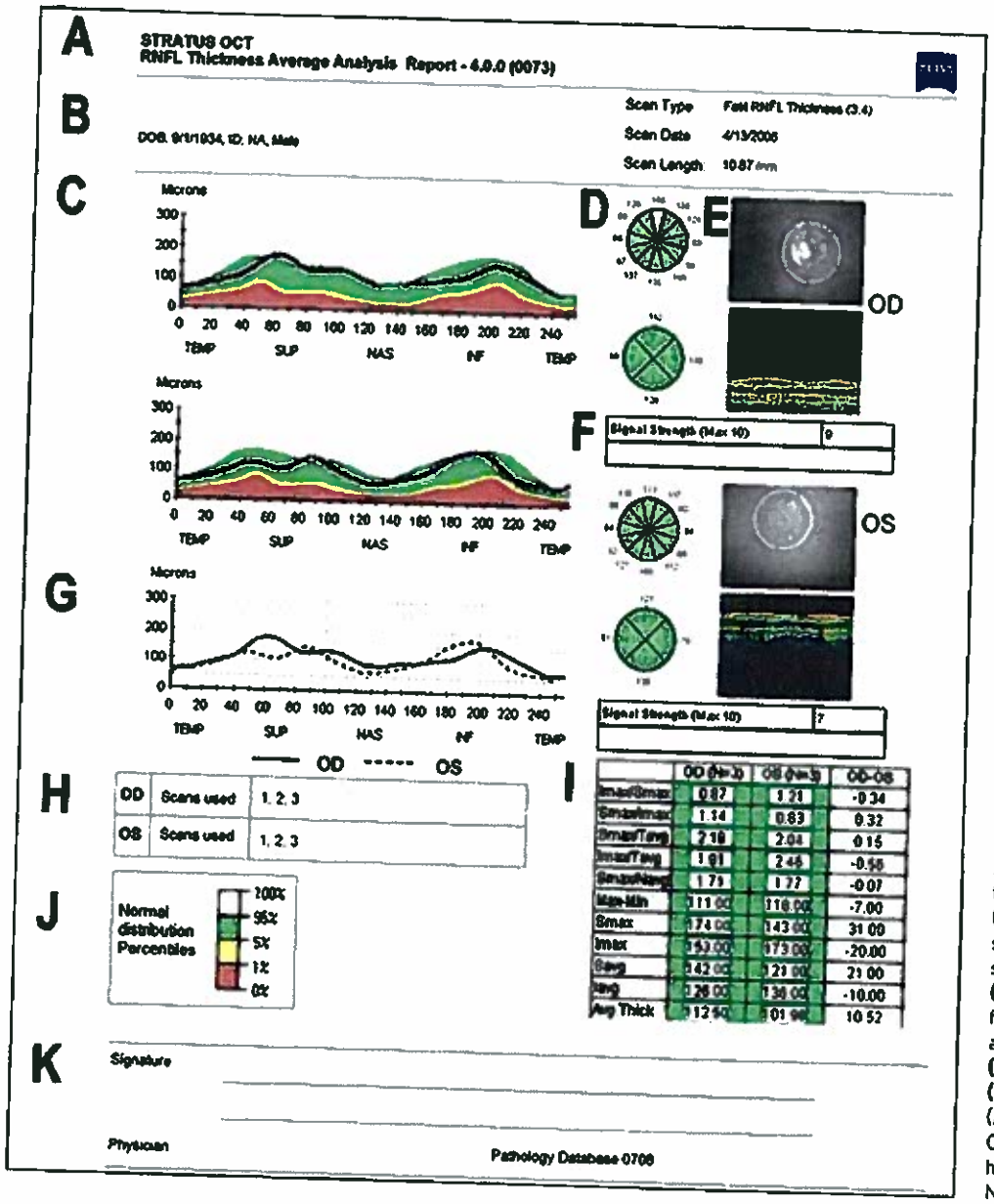

Fig. 14-13 OCT RNFL thickness average analysis report. **(A)** Type of report. **(B)** Patient information. **(C)** RNFL thickness graph with color-coded normative database. **(D)** Clock-hour thickness (top) and quadrant thickness (bottom) **(E)** Fundus image showing scan placement (top) and single OCT scan (bottom). **(F)** Signal strength. **(G)** Overlay graph of RNFL thickness for both eyes. **(H)** Scans included in analysis. **(I)** Measured parameters. **(J)** Percentiles for normal distribution. **(K)** Physician interpretation. (Adapted from Schuman JS, Puliafito CA, Fujimoto JG: Everyday OCT: a handbook for clinicians and technicians. NJ, USA, Slack Inc., 2006.)[24]

ONH scan

The same 'star' or 'spoke' pattern scan used to scan the macula is also used to scan the ONH. Each line measures 4 mm in this linear scan. Optical coherence tomography automatically defines the ONH margin as the endings of the RPE, which are marked by a blue cross. A straight line is drawn connecting these crosses. A parallel line is drawn 150 microns anterior to this line. This line is analogous to the reference plane described in HRT. Anything above the line is considered rim and anything below is considered cup.

Fast scans

These are available with OCT 3. They are time efficient, obtained in 1.92 seconds. Accuracy of the scan is improved secondary to reduction of error caused by the patient's movement or loss of fixation. Resolution is lower. All three structures (RNFL, macula, and ONH) can be scanned using the 'fast-scan' modality.

Comparison of three scanning areas has been done. Stratus OCT (OCT 3) demonstrated reproducible measurements of RNFL, macular and ONH parameters in one study.[25] In a comparison for detection of glaucoma damage, OCT ONH and RNFL parameters proved to be superior than macular parameters in discriminating normal from glaucoma patients.[26]

COMPONENTS OF THE OCT REPORT

RNFL thickness average analysis

The printout includes RNFL thickness curves for both eyes. The RNFL curve is drawn as a black line on a graph featuring thickness in microns and different areas of the peripapillary RNFL: temporal, superior, nasal, and inferior. The RNFL curve is drawn over a background of color-coded (green means within normal limits, yellow means borderline and red means outside normal limits) shaded

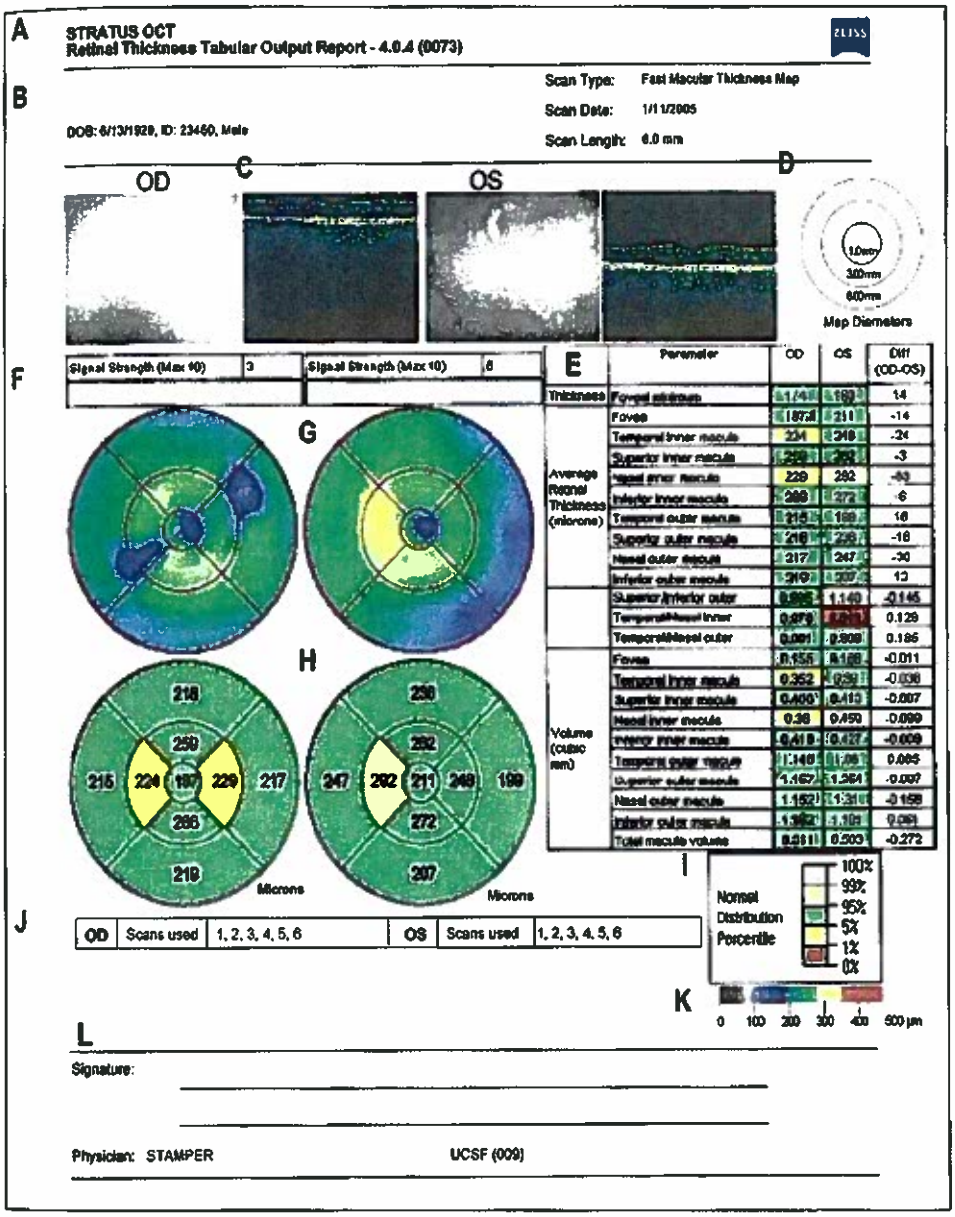

Fig. 14-14 Retinal thickness tabular output report. **(A)** Type of report. **(B)** Patient and scan information. **(C)** Fundus image and single OCT scan. **(D)** Diameters used for thickness map. **(E)** Thickness and volume parameters. **(F)** Signal strength. **(G)** Color-coded thickness map. **(H)** Thickness map with normative data. **(I)** Percentiles for normal distribution. **(J)** Scans included in the analysis. **(K)** Color-coded thickness scale. **(L)** Physician interpretation. (Adapted from Schuman JS, Puliafito CA, Fujimoto JG: Everyday OCT: a handbook for clinicians and technicians. NJ, USA, Slack Inc., 2006.)[24]

areas representing RNFL thickness classification according to the normative database. A normal RNFL curve will have the characteristic 'double hump' appearance with the superior and inferior RNFL being thicker than the nasal and temporal RNFL. The peripapillary RNFL is divided into 12 clock hours and into four quadrants. All are classified in a color-coded manner. A photo of the retina while the scan was obtained is also shown in the printout. The circular scan appears in the picture and its centration over the ONH can be corroborated. Centration is important for accurate thickness measurements of all quadrants. A false color cross-sectional image is shown for both eyes with signal strengths specified for each image. The average thickness is calculated for both eyes and it appears at the bottom of the thickness measurement table. The thickness values are color coded as well. Studies have been done to assess the reproducibility of these values. Schuman et al.[27] found a SD of 10–20 microns for the average RNFL thickness and 15–30 microns for the clock-hour measurements (Fig. 14-13).

Macular analysis

A retinal thickness analysis and a retinal map analysis can be obtained from the macular scan data. The retinal thickness printout provides a cross-sectional image of the retina along a specific axis of scan (indicated in the printout), signal strength, and a thickness chart with background shaded areas representing the normative database. A retinal thickness measurement is also provided. The retinal map analysis also provides a cross-sectional image and includes two maps, one with qualitative and another with quantitative thickness measurements. Measurements for nine macular sectors are shown as well as thickness measurements for the center of the scan and the total macular volume (Fig. 14-14).

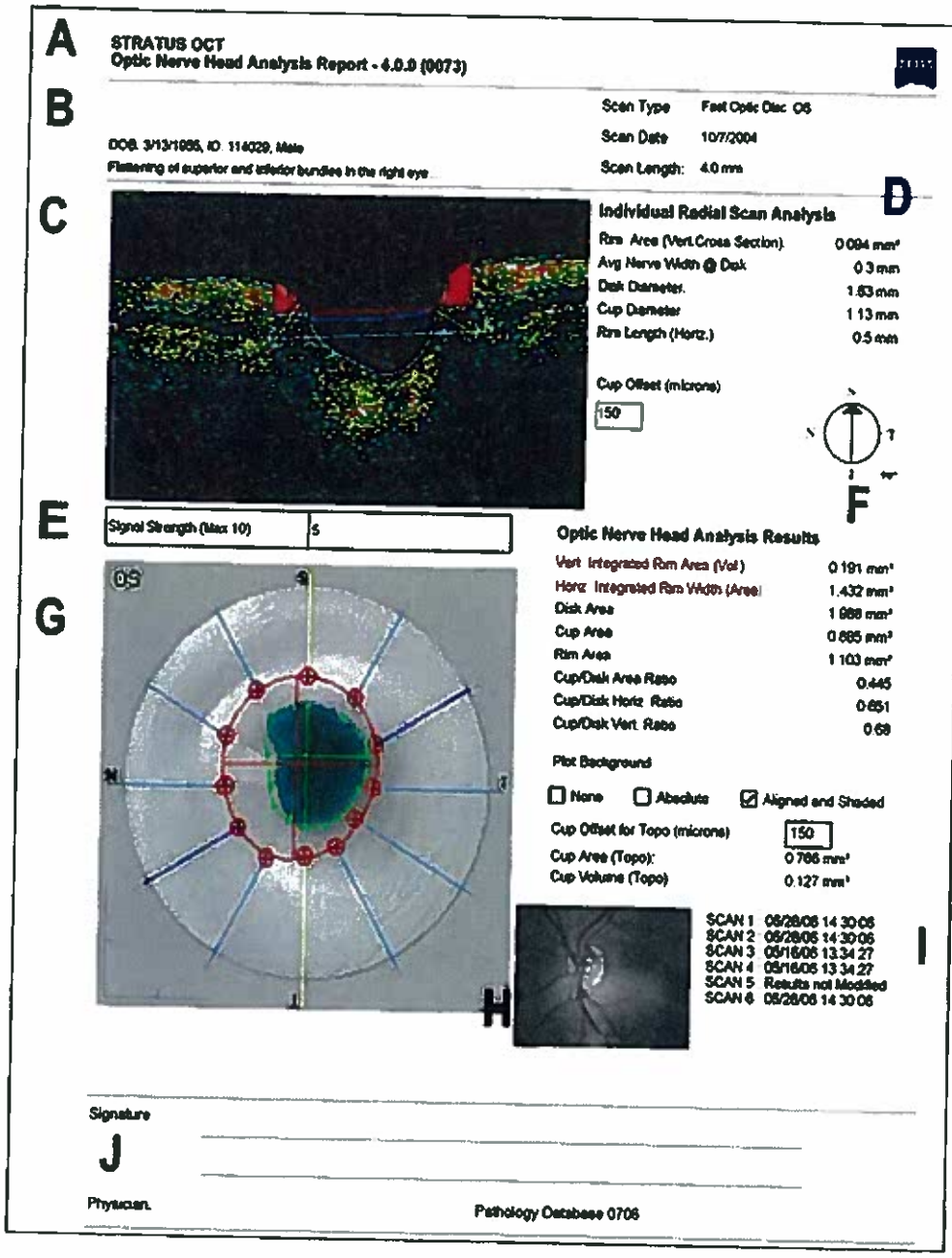

Fig. 14-15 Optic nerve head analysis report. **(A)** Type of report. **(B)** Patient and scan information. **(C)** Single OCT image. **(D)** Single scan analysis parameters. **(E)** Signal strength. **(F)** Overall analysis parameters. **(G)** Plot of radial scans with selected scan indicated by yellow lines. **(H)** Fundus image showing scan placement. **(I)** Times at which the radial scan was last modified. **(J)** Physician interpretation.
(Adapted from Schuman JS, Puliafito CA, Fujimoto JG: Everyday OCT: a handbook for clinicians and technicians. NJ, USA. Slack Inc., 2006.)[24]

Optic nerve head analysis

A false color cross-sectional image of the optic nerve head is presented and is overlaid with two horizontal lines: one connects the edges of the RPE together and the other represents the reference plane. Tissue located above the reference plane and within the edges of the RPE is considered neuroretinal rim, and tissue below the reference plane and within the edges of the RPE is considered cup. The area corresponding to the rim is colored in red, the contour is traced in green and the edge of the ONH, which is defined automatically by the OCT as the termination of the RPE is traced, in yellow. Such contours of the optic nerve are drawn beside the previous image. Information on all six radial scans is used for the contour of the ONH. One of the radial scans is yellow and it represents the axis of the cross-sectional image in the printout (Fig. 14-15).

QUALITY ASSESSMENT

- *Peripapillary circular scan centration*: decentration of the scan can account for inaccurate measurements of RNFL thickness. For example, if the circle is displaced inferiorly, the superior sector will be thicker than if the scan was centered and the inferior quadrant might be measured thinner than the real thickness. The RNFL that is closer to the disc will be thicker than further way.
- *Signal strength value*: the manufacturer suggests a signal strength not lower than 5. Signal strength equal to or stronger than 6 is considered to indicate good quality.
- *Homogeneity of the RNFL scan*: loss of reflectivity in the scan is less than ideal and can affect the overall quality.
- *OCT algorithm*: the RNFL is usually shown in between two white lines that delineate its anterior and posterior borders.

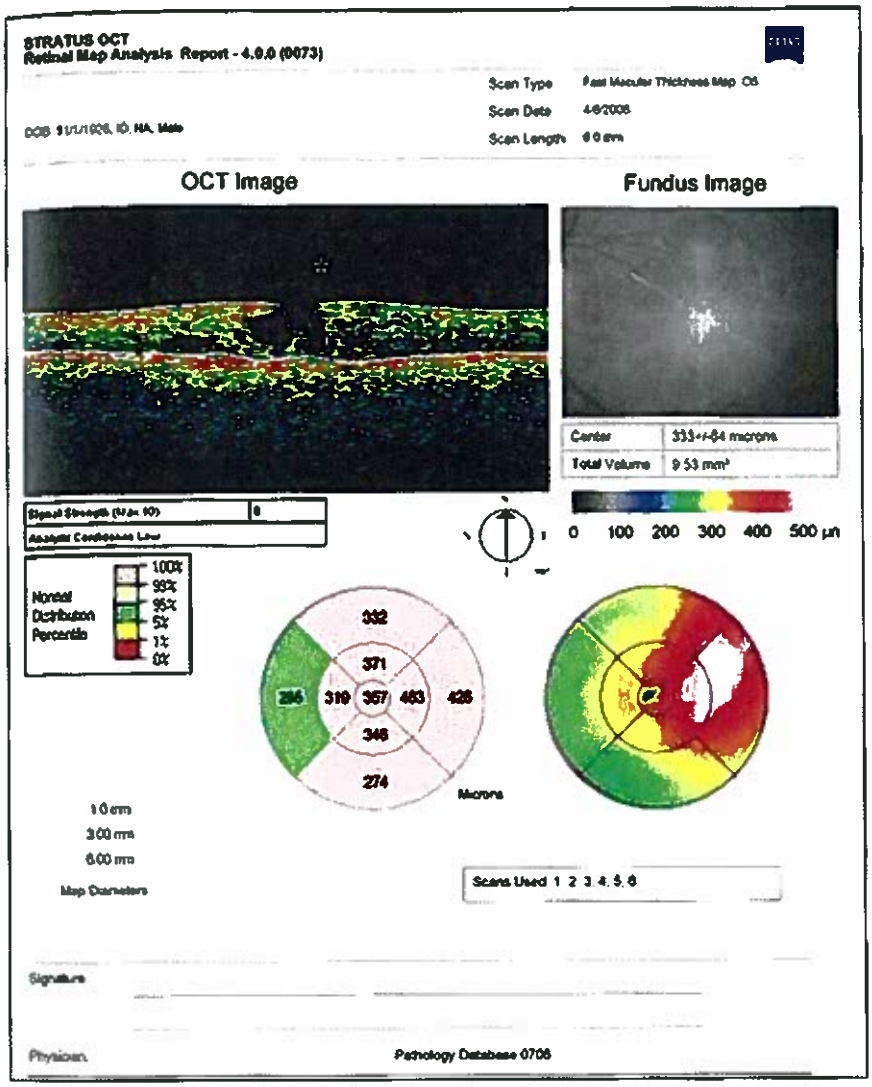

Fig. 14-16 Example of algorithm failure of the macular scan, as evidenced by disrupted image (*).
(Courtesy of Zeiss Meditec, Inc., Jena, Germany.)

Sometimes, in poor quality scans, the white lines fail to follow the limits of the RNFL and a 'dropout' is seen in the cross-sectional image (Fig. 14-16).

STRENGTHS AND LIMITATIONS

Optical coherence tomography is the most versatile ancillary imaging test used in ophthalmology. It has the best axial resolution of all imaging devices and provides images of such high resolution that cross-sections of tissues can be compared to histopathology slides. *It is also the only technology capable of imaging the RNFL, macula and ONH.* Compared to HRT, OCT is obtaining thickness measurements and not height measurements. Insofar as OCT macular imaging has opened the doors to a better understanding, diagnosis and follow-up of innumerable retinal pathologies assessment of the macular region by OCT holds promise in detecting early glaucomatous changes as well.[27b] As with the other devices, it is a machine that is easy to operate, safe and can obtain images without pupillary dilation.

Limitations include its normative database, and its limited sampling density that reduces its transverse resolution. Of note is that a newer generation of OCT (Spectral OCT) will provide higher resolution and three-dimensional images. Another limitation is that OCT data are originated from one set of scans and not a series (three) of sets of scans as in HRT. And unlike the HRT 3, current OCT devices have not yet developed robust programs for the longitudinal evaluation of glaucomatous progression..

TESTING FROM THE PATIENT'S PERSPECTIVE

Patients will be asked to place their chin in the chin rest and forehead against the headrest. Again, the exam feels similar to the slit-lamp exam. The patient will see different light patterns as the OCT comes into position for the scan: glowing red scan pattern, red landmark spot and green fixation target. If the patient has a cata ract, he or she may perceive the green light as being white or yellow. There is the option of using an external fixation wand for the fellow eye which is useful when the eye being scanned is blind and cannot hold fixation with the internal light.

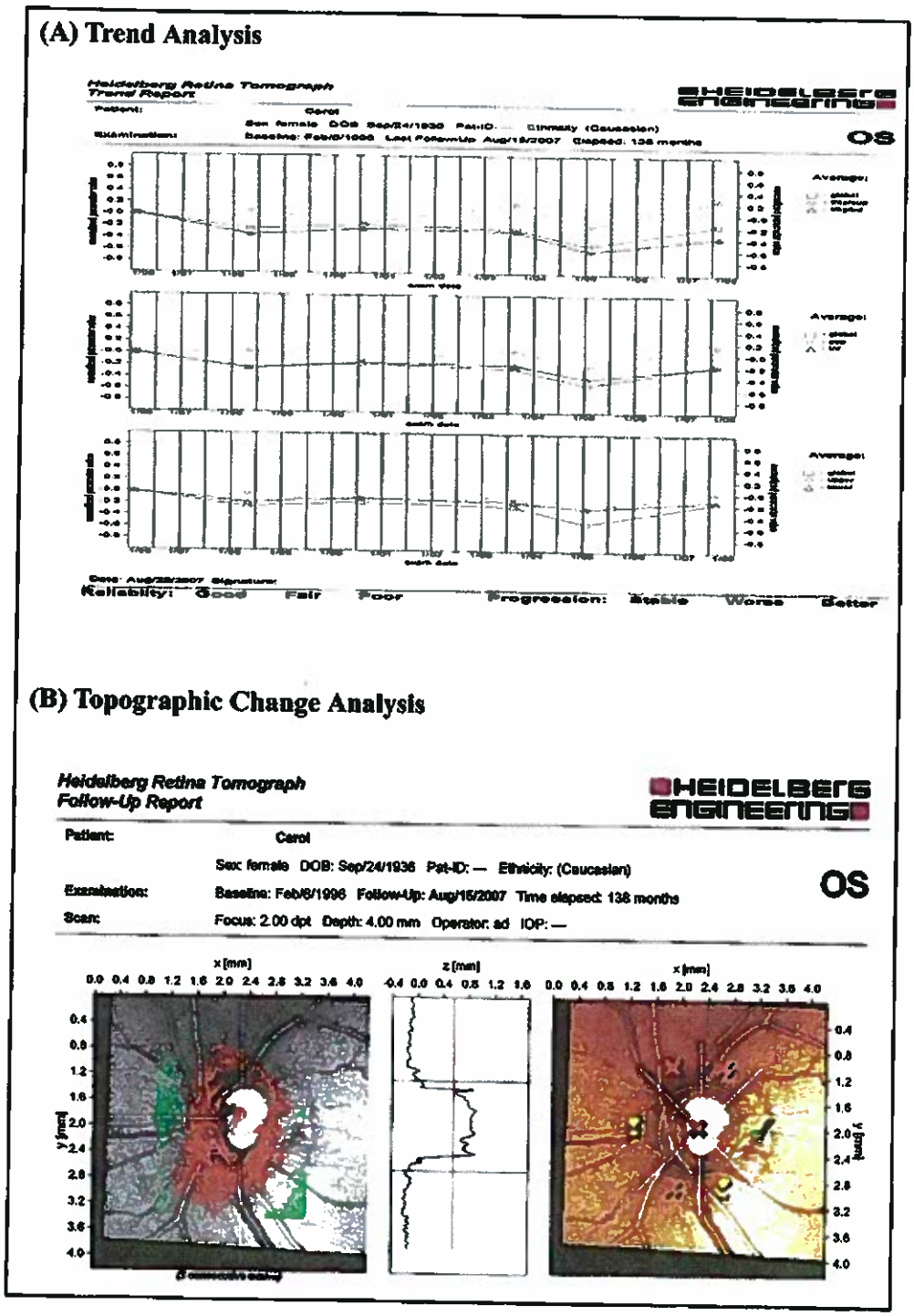

Fig. 14-17 Change analysis with HRT. **(A)** Trend analysis: several parameters are plotted over time giving a linear indication of progression. **(B)** Alternatively, topographic change analysis (TCA) can be used to evaluate for glaucoma progression. Change probability maps with red or green over the optic nerve image indicate change in topography having significant *P* values. Red means depression and green elevation. Note that for the same patient, trend analysis appears stable but rim seems to be depressed.

LONGITUDINAL EVALUATIONS

To assess change over time, HRT uses what is called the topographic change analysis or TCA.[28] This is a statistical method to compare topographic values of superpixels over time. It calculates the probability (*P* value) of the difference in height values between two time points to be caused by chance alone. A high *P* value ($P > 0.05$) would indicate high probability of the change to be caused by chance, and a low *P* value ($P < 0.05$) would mean that the change did not occur by chance. Topographic change analysis is automatically done after the third scan is obtained: one baseline and two follow-up scans. The analysis is made with raw topographic values, so it is independent of disc contour delineation. The display occurs as a change probability map with the reflectivity maps overlaid with color-coded superpixels that had significant *P* values of change. Red means depression and green means elevation (Fig. 14-17).

The RNFL thickness longitudinal evaluation with OCT has been explored in recent studies. Wollstein et al compared the ability

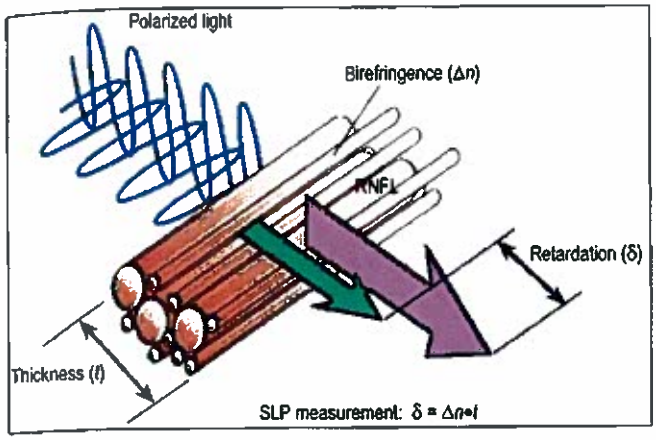

Fig. 14-18 In the retina, the parallel arrangement of the microtubules in retinal ganglion cell axons causes a change in the polarization of light passing through them. The change in the polarization of light is called retardaxtion and it can be quantified. The retardation value is proportionate to the thickness of the RNFL.

of peripapillary RNFL measurements obtained by OCT, visual fields and clinical assessment of detecting progression in glaucoma suspects and glaucoma patients.[29] Investigators found that a greater likelihood of glaucomatous progression was identified by OCT versus automated perimetry.

SCANNING LASER POLARIMETRY

GDX

Scanning laser polarimetry is an imaging technology that is utilized to measure peripapillary RNFL thickness. It is based on the principle of birefringence. The main birefringent intraocular tissues are the cornea, lens and the retina. In the retina, the parallel arrangement of the microtubules in retinal ganglion cell axons causes a change in the polarization of light passing through them. The change in the polarization of light is called retardation, which can be quantified. The retardation value is proportionate to the thickness of the RNFL (Fig. 14-18). GDX is the device that utilizes this technology.

The latest generation is the GDX variable corneal compensator (GDX VCC, Carl Zeiss Meditec; Jena, Germany, and Dublin, California) (Fig. 14-19). This device also uses a diode laser (780 nm) to obtain measurements along a 15 × 15 area of the retina. The scan is obtained by the use of an ellipse that must be centered over the ONH as seen in the reflectance map. Data from the scanned area are displayed as a 256 × 256 pixel color-coded grid, representing different levels of retardation and therefore RNFL thickness. A retardation map and a deviation map are included in the printout.

VCC stands for variable corneal compensator, which was created to account for the variable corneal birefringence in patients. It uses the birefringence of Henle's layer in the macula as a control for measurement of corneal birefringence. Birefringence around the fovea is known to be uniform and arises from Henle's layer. Scanning laser polarimetry of the macula with no compensation for the anterior segment gives rise to a non-uniform pattern at the fovea due to birefringence of the cornea, and the hourglass pattern indicates the axis and magnitude of the uncorrected cornea birefringence (Fig. 14-20).

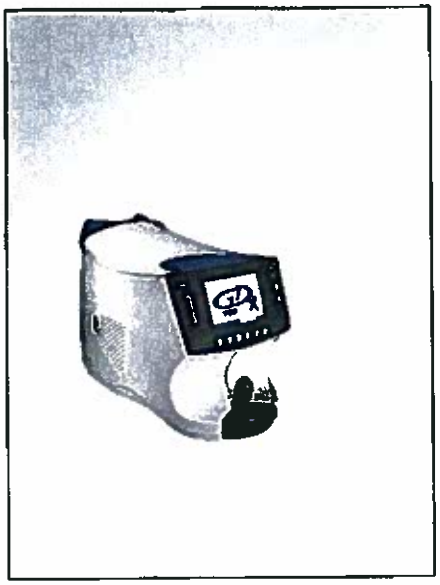

Fig. 14-19 GDX VCC imaging unit.
(Courtesy of Zeiss Meditec, Inc., Jena, Germany.)

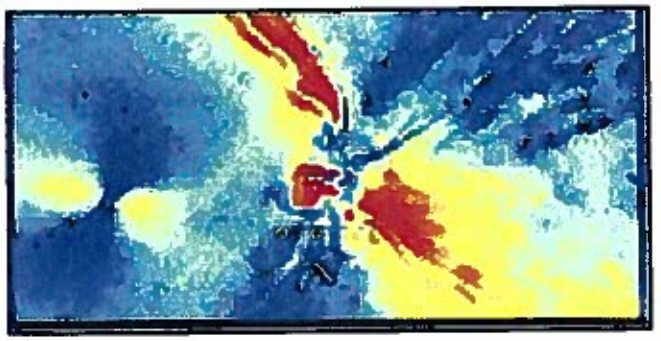

(A)

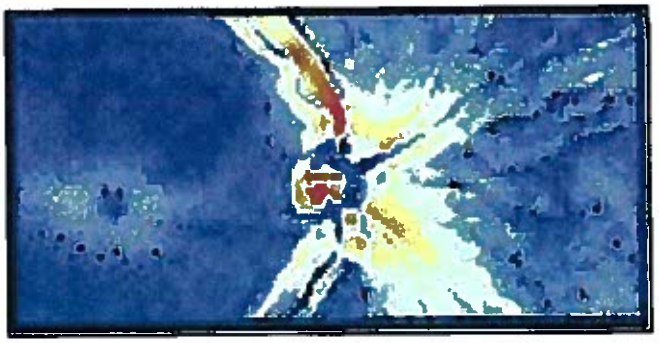

(B)

Fig. 14-20 Birefringence around the fovea is uniform and arises from Henle's layer. When a 'bow-tie' or 'hourglass' shape is seen around the fovea, this represents corneal birefringence. The bow-tie's magnitude and axis is representative of corneal birefringence.
(A) Depicts an example of corneal birefringence before compensation, and **(B)** shows the d ssapearance of the bow-tie after corneal compensation has been made

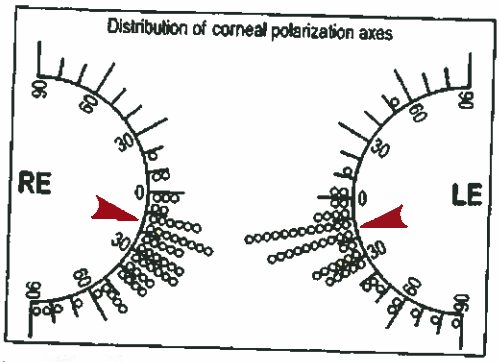

Fig. 14-21 Variability in magnitude and axis of corneal birefringence is significant and therefore there is the advantage of using a variable corneal compensator (VCC) as opposed to the previous fixed corneal compensator.

The VCC was incorporated after noticing a large variability in corneal birefringence among different patients and acknowledging the fact that a fixed generic corneal compensator was not going to suffice (Fig. 14-21).[30] An enhanced corneal compensator (ECC) with some improved features over VCC is currently being tested. One recent study reported that ECC significantly reduces the frequency and severity of atypical birefringence patterns compared with VCC and improves the correlation between RNFL measures and visual function.[31]

Components of the GDX report

1. *Patient data and quality score:* the patient's name, date of birth, gender and ethnicity are reported at the top of the printout. An ideal quality score is from 7 to 10 (Fig. 14-22).
2. *Fundus image:* it is a reflectance image of the posterior pole that measures 20° by 20° (Fig. 14-23). GDX VCC obtains more than 16 000 data points to construct this image. During the scanning process, this image serves to evaluate the quality of the scan before moving forward. Also, the operator centers the ellipse over the ONH in this image. The ellipse size is defaulted to a small setting but manipulating the calculation circle can change the size of the ellipse. The calculation circle is the area found between the two concentric circles, which measure the temporal-superior-nasal-inferior-temporal (TSNIT) and nerve fiber indicator (NFI) parameters. By resizing the calculation circle and ellipse, the operator is able to measure beyond a large peripapillary atrophy area, for example (Fig. 14.24).
3. *RNFL thickness map:* this is a color map depicting the different thicknesses of peripapillary RNFL (see Fig. 14-23). It represents the retardation level of the different scanned points. Hot colors like red and yellow mean high retardation or thicker RNFL and cool colors like blue and green mean low retardation or thinner areas. A typical scan pattern is that one with thicker RNFL superiorly and inferiorly, like a vertical bow-tie (Fig. 14-25).
4. *TSNIT graph:* this graph demonstrates the patient's RNFL thickness as a black line drawn over a shaded area of normality based on a normative database of over 500 eyes. This graph is based on data points within the calculation circle.
5. *TSNIT symmetry graph:* this graph overlays the individual TSNIT graphs for the right and left eye.
6. *TSNIT comparison graph and serial analysis graph:* these graphs compare two or more scans of the same eye obtained on different visits. These graphs do not appear on the regular printout.
7. *Deviation from normal map:* this map shows how the patient's RNFL thickness compares with the values derived from the normative database. Color-coded squares indicate the amount of deviation from normal at each given location. A color legend defining statistical significance of deviation from normal appears at the bottom (see Fig. 14-23).
8. *TSNIT parameters:* these are computed from the calculation circle data and are compared to the normative database. They are also color coded based on different *P* values. The parameters are TSNIT average (average thickness values within the calculation circle), superior average (average of pixels in superior 120° of the calculation circle), inferior average (same as above, but along the inferior 120°), TSNIT standard deviation and inter-eye asymmetry.
9. *Nerve fiber indicator (NFI):* the NFI is an indicator of the likelihood that an eye has glaucoma. It is a proprietary value, so its exact origin has not been published. Data within and outside the calculation circle are used to generate the NFI value. It is a number between 0 and 100. The higher the NFI, the more likely the patient has glaucoma. The GDX manufacturer offers the following as a guideline on the NFI interpretation:
   - <30: low likelihood of glaucoma
   - 30–50: glaucoma suspect
   - >50: high likelihood of glaucoma.

Quality assessment

- Appropriate focusing and illumination of the retinal area being scanned is necessary.
- The ONH must be inside a black square while obtaining the scan.
- Presence of motion artifacts can decrease the quality of the scan. These are sometimes noticed as black rectangles at the edges of the scans or lines along the vessels.
- The ellipse must be centered over the ONH. Centration is usually more important than adequate size.
- The scan will provide a 'quality score.' A score between 7 and 10 is ideal. The device will also provide 'OK' for alignment, fixation and refraction (Fig. 14-26).
- Presence of atypical scans in the retardation map. A typical scan should have the thicker bundles along the vertical axis, where the RNFL is thicker. The pattern of a normal RNFL should be that of a vertical bow-tie. An atypical scan is one where the overall thickness is increased, where the thickness axis is tilted or where the thickness is along radial lines through the periphery of the scan. An objective way to evaluate atypical scans is with a support vector machine, which assigns a typical scan score.

Strengths and limitations

GDX allows for rapid and simple imaging of peripapillary RNFL. Good interactive features to assess for quality of the image are included in the software. As with the previous technologies, no papillary dilation is necessary. This device can only provide RNFL data. Corneal surgery will induce error in the measurements, but these should be corrected by VCC. On the other hand, macular pathology is likely to impede GDX scanning, given that VCC calculation is dependent on an intact Henle's layer. The NFI or likelihood score for having glaucoma is a proprietary value and cannot be independently validated.

Studies have been published demonstrating GDX reproducibility and use in glaucoma evaluation, but most of the published studies were done with the fixed corneal compensator used in the earlier

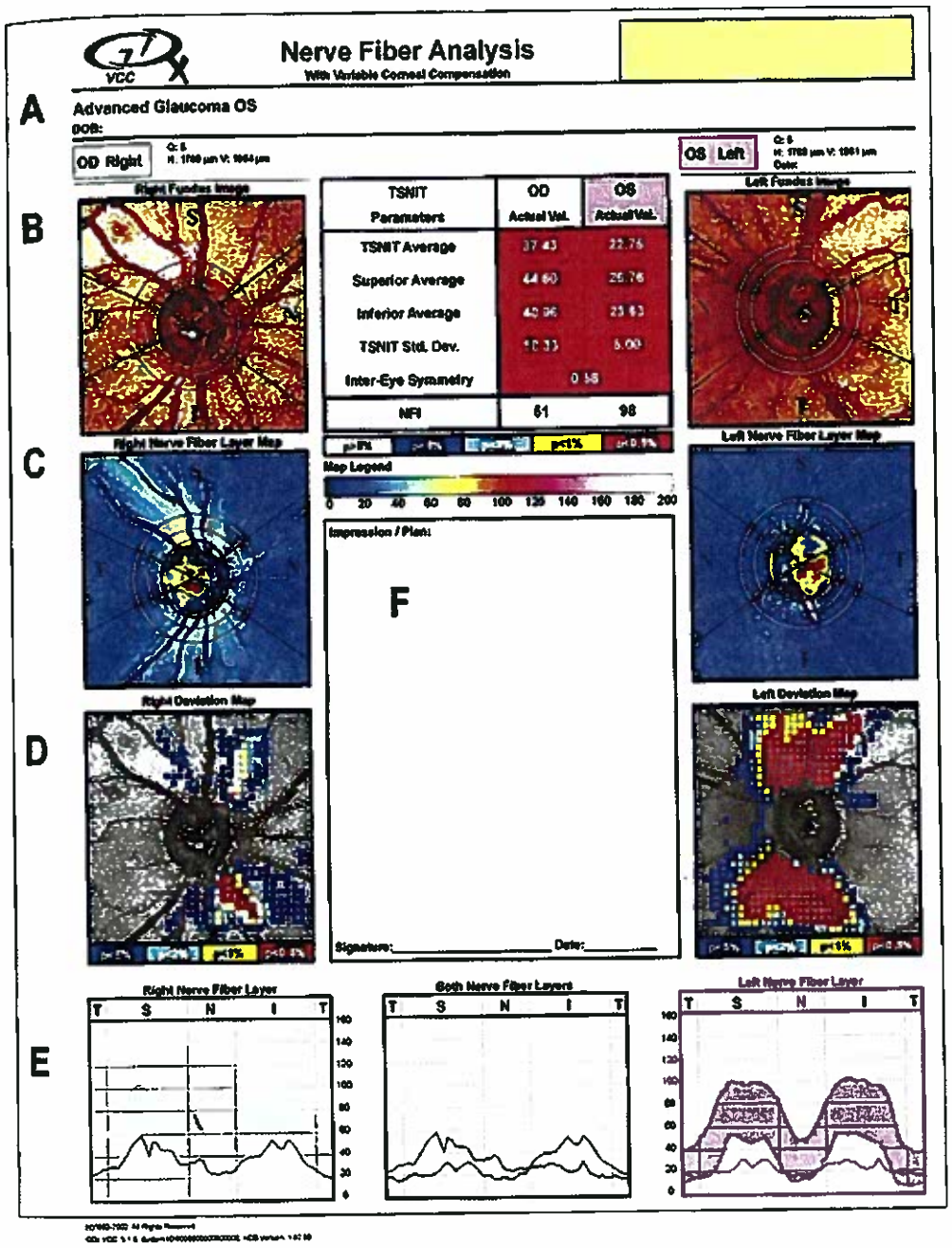

Fig. 14-22 GDX printout **(A)** Patient and quality information. **(B)** This shows the reflectance image and a table with temporal-superior-nasal-inferior-temporal (TSNIT) and nerve fiber indicator (NFI) parameters for each eye. **(C)** This consists of the retardation or RNFL thickness maps, which are color coded with hot colors representing thicker RNFL. **(D)** These are the deviation plot maps. Each small square is color coded and represents deviation from normality. The color represents the *P* value for abnormal points. **(E)** TSNIT and TSNIT symmetry maps show the patient's RNFL curve or curves against a shaded area representing the normative database **(F)** Space for physician interpretation Note the asymmetry between right and left eye, with the left eye having a much thinner nerve fiber layer. (Courtesy of Zeiss Meditec, Inc., Jena, Germany.)

generation of GDX.[32-34] Reports do exist evaluating GDX VCC in different circumstances, such as presence of peripapillary atrophy[35] or in comparison to HRT and OCT.[36-38]

Testing from the patient's perspective

The patient will be asked to place his or her face into the 'mask' of the GDX. The patient will see a field of thin red horizontal lines. On one side of the field, the patient will see short, bright, blinking red horizontal lights similar to an equal sign. That is the patient's fixation target. The scan acquisition takes less than 1 second.

CONCLUSIONS

Glaucomatous changes can affect the optic nerve structure and its function. For the most part, optic nerve structural changes frequently precede functional changes. Thus the ability to detect early glaucomatous structural changes has great potential value in delaying and avoiding progression of the disease. This chapter has reviewed the most important imaging devices currently (2007) used in the evaluation of glaucoma. They have been of enormous value in the comprehension and evaluation of glaucomatous

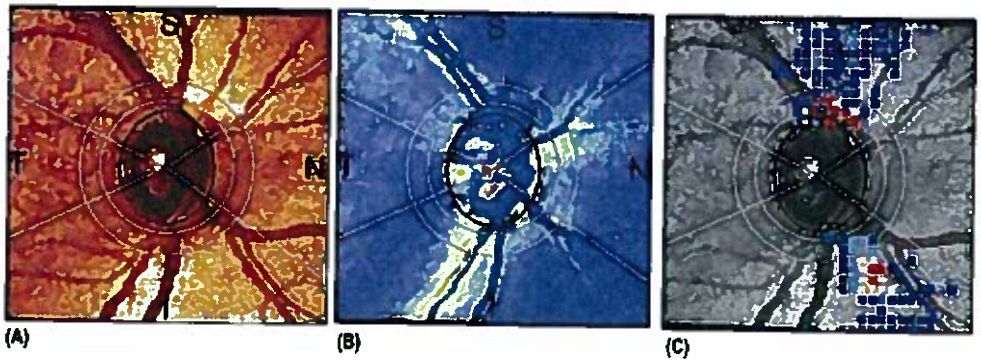

Fig. 14-23 Different peripapillary images in GDX report. From left to right: reflectance image with the ellipse centered on the disc, retardation or RNFL thickness color map and deviation plot.
(Courtesy of Zeiss Meditec, Inc., Jena, Germany.)

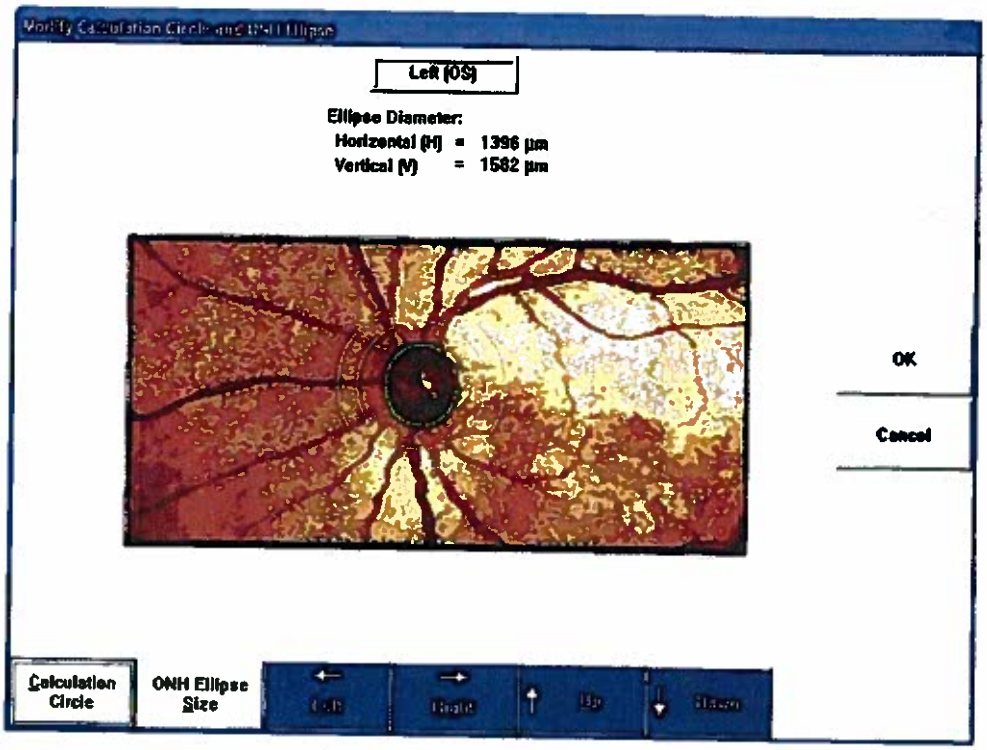

Fig. 14-24 Operator's screen during GDX scanning of a patient. The operator places the ellipse over the ONH. It must be centered appropriately. The calculation circle is the area between the two concentric circles and it can be modified by the operator. Manipulating the calculation circle allows for resizing of the ellipse. TSNIT parameters are derived from measurements of RNFL within the calculation circle and NFI parameters are derived from RNFL inside and outside the calculation circle.
(Courtesy of Zeiss Meditec, Inc., Jena, Germany.)

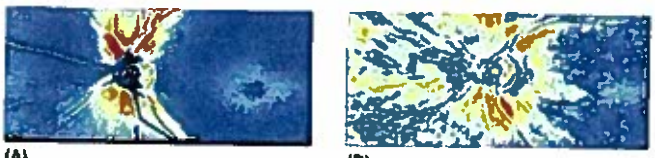

Fig. 14-25 Typical and atypical GDX scans. Typical scans will show a vertical bow-tie, with thicker RNFL (hot colors) superiorly and inferiorly such as the scan seen in **(A)**. **(B)** is an example of an atypical scan, showing increased overall thickness.

disease during the last couple of decades. Some of these have been used as ancillary tools in relevant clinical trials.

Despite their advantages, there are important limitations. None of these devices has the ability to specifically capture all the nuances of appearance available in stereoscopic photographs of the disc, and which can serially be examined by the clinician with a low-tech light box. Given the rapid and unpredictable innovation in preferred and compatible technologies of optic nerve imaging which may make earlier studies uninterpretable a decade hence – many clinicians would do well to obtain baseline disc photographs

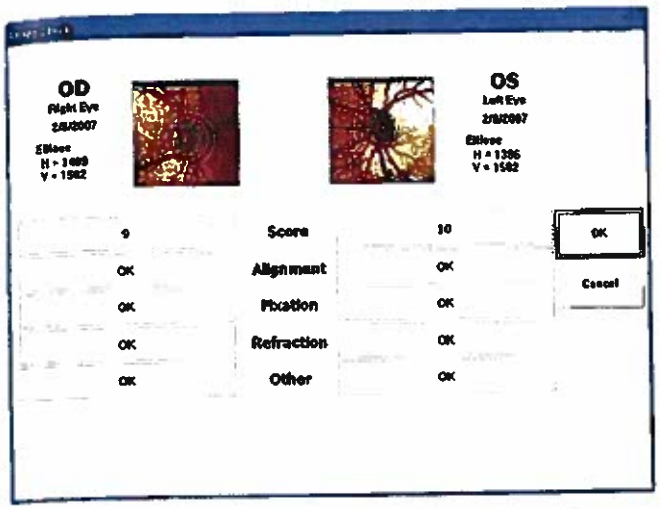

Fig. 14-26 Image quality check screen while scanning a patient with GDX.

on all glaucoma patients. Another unavoidable frustration, besides rapidly changing technologies, is the clinical fact that the most difficult optic discs to interpret in terms of glaucomatous changes – specifically highly myopic and tilted optic discs – are also those discs which optic nerve imaging devices have the greatest limitations in discriminating abnormality from pathology.

Hence these devices should not be regarded as replacing the skilled ophthalmologist's capacity to evaluate all aspects of the patient's diagnosis and disease status but they can definitely aid in the complicated decision-making process that is so commonly involved in glaucoma practice. Imaging technology has made a gigantic contribution to glaucoma by providing objective parameters, but care should be taken in analyzing these tests, remembering that test quality and reliability need to be assessed before interpreting them.

REFERENCES

1. American Academy of Ophthalmology: Basic and clinical science course. Glaucoma, San Francisco, American Academy of Ophthalmology. 2006.
2. Quigley HA, et al: An evaluation of optic disc and nerve fiber layer examinations in monitoring progression of early glaucoma damage. Ophthalmology 99:19, 1992.
3. Weinreb RN, Greve EL, editors: Glaucoma diagnosis: structure and function, Amsterdam, Kugler, 2004.
4. Lichter PR: Variability of expert observers in evaluating the optic disc. Trans Am Ophthalmol Soc 74:532, 1976.
5. Gaasterland DE, et al: Advanced Glaucoma Intervention Study Investigators: The Advanced Glaucoma Intervention Study (AGIS: 10 Variability among academic glaucoma subspecialists in assessing optic disc notching. Trans Am Ophthalmol Soc 99:177, 2001.
6. Chen PP: Blindness in patients with treated open angle glaucoma, Ophthalmology 110:726, 2003.
7. Hattenhauer MG, et al: The probability of blindness from open angle glaucoma. Ophthalmology 105:2099, 1998.
8. Zangwill LM, et al: Optic nerve imaging: recent advantages, In: Grehn F, Stamper R, editors Glaucoma, Berlin, Springer-Verlag, pp 63–91, 2004.
9. Fingeret M, Flanagan JG, Liebman JM. The essential HRT primer. USA, Heidelberg Engineering, p. 2, 2005.
10. Zangwill LM, et al: The confocal scanning laser ophthalmoscopy ancillary study to the ocular hypertension treatment study: a study design and baseline factors, Am J Ophthalmol 137:219, 2004.
11. Zangwill LM, et al: Racial differences in optic disc topography: baseline results from the confocal scanning laser ophthalmoscopy ancillary study to the ocular hypertension treatment study: a study design and baseline factor. Am J Ophthalmol 122:22, 2004.
12. Hatch WV, et al: Interobserver agreement of Heidelberg retina tomography parameters, J Glaucoma 8:232, 1999.
13. Jonas JB, Mardin CY, Grundler AE: Comparison of measurements of neuroretinal rim area between confocal laser scanning tomography and planimetry of photographs, Br J Ophthalmol 82:362, 1998.
14. Dichtl A, Jonas JB, Mardin CY: Comparison between tomographic scanning evaluation and photographic measurement of the neuroretinal rim. Am J Ophthalmol 121:494, 1996.
15. Camejo L, et al: Evaluation of Heidelberg retina tomography (HRT 3) in healthy eyes, Invest Ophthalmol Vis Sci 47, 2006 E abstract 3632.
16. Burgansky ZE, et al: Detecting glaucoma with Heidelberg retina tomograph 3 (HRT 3), Invest Ophthalmol Vis Sci 47, 2006 E-abstract 3630.
17. Bilonick RA, et al: Heidelberg retina tomograph (HRT) II vs. HRT 3: what is the difference?, Invest Ophthalmol Vis Sci 47, 2006. E-abstract 3633.
18. Hatch WV, et al: Laser scanning tomography of the optic nerve head in ocular hypertension and glaucoma, Br J Ophthalmol 81:871, 1997.
19. Iester M, et al: A comparison of healthy, ocular hypertensive, and glaucomatous optic disc topographic parameters, J Glaucoma 6 363, 1997
20. Mikelberg FS, Parfitt CM, Swindale NV: Ability of the Heidelberg retina tomograph to detect early glaucomatous visual field loss, J Glaucoma 4:242, 1996.
21. Wollstein G, Garway-Heath DF, Hitchings RA Identification of early glaucoma cases with the scanning laser ophthalmoscope. Ophthalmology 105:1557, 1998.
22. Fujimoto JG, et al: Optical coherence tomography: an emerging technology for biomedical imaging and optical biopsy. Neoplasia 2 9, 2000
23. Fujimoto JG: Optical coherence tomography for ultrahigh resolution in vivo imaging, Nat Biotechnol 21:1361, 2003.
24. Schuman JS, Puliafito CA: Fujimoto JG Everyday OCT: a handbook for clinicians and technicians, NJ, USA, Slack Inc., 2006.
25. Paunescu LA, et al: Reproducibility of nerve fiber thickness, macular thickness and optic nerve head measurements using StratusOCT, Invest Ophthalmol Vis Sci 45:1716, 2004.
26. Wollstein G, et al: Comparison of three optical coherence tomography scanning areas for detection of glaucomatous damage, Am J Ophthalmol 139:39, 2005.
27. Schuman JS, et al: Reproducibility of nerve fiber layer thickness measurements using optical coherence tomography, Ophthalmology 115: 949–956, 2008.
27b. Tan O, Li G, Lu AT: Mapping of macular substructures with optical coherence tomography for glaucoma diagnosis. Ophthalmology 103:1889, 1996.
28. Chauhan BC, et al: Technique for detecting serial topographic changes in the optic disc and peripapillary retina using scanning laser tomography, Invest Ophthalmol Vis Sci 41:775, 2000.
29. Wollstein G, et al: Optical coherence tomography longitudinal evaluation of retinal nerve fiber layer thickness in glaucoma, Arch Ophthalmol 123:464, 2005.
30. Greenfield DS, Knighton RW, Huang XR. Effect of corneal polarization axis on assessment of retinal nerve fiber layer thickness by scanning laser polarimetry, Am J Ophthalmol 129:715, 2005.
31. Sehi M, et al: Advanced Imaging in Glaucoma Study Group: Scanning laser polarimetry with variable and enhanced corneal compensation in normal and glaucomatous eyes, 143:272, 2007.
32. Xu L, et al: Quantitative nerve fiber layer measurement using scanning laser polarimetry and modulation parameters in the detection of glaucoma, J Glaucoma 7:270, 1998.
33. Bowd C, et al: Detecting early glaucoma by assessment of retinal nerve fiber layer thickness and visual function, Invest Ophthalmol Vis Sci 42:1993, 2001.
34. Choplin NT, Lundy DC: The sensitivity and specificity of scanning laser polarimetry in the detection of glaucoma in a clinical setting, Ophthalmology 108:899, 2001.
35. Kunimatsu S, et al: Performance of GDX VCC in eyes with peripapillary atrophy: comparison of three circle sizes, Eye 22:173, 2008. Epub Aug 4 2006
36. Zangwill LM, et al: Discriminating between normal and glaucomatous eyes using the Heidelberg Retina Tomograph, GDX Nerve Fiber Analyzer, and Optical Coherence Tomograph, Arch Ophthalmol 119 985, 2001.
37. Brusini P, et al: Comparison between GDx VCC scanning laser polarimetry and Stratus OCT optical coherence tomography in the diagnosis of chronic glaucoma, Acta Ophthalmol Scand 84:650, 2006.
38. Hong S, et al: Early glaucoma detection using the Humphrey Matrix Perimeter, GDx VCC, Stratus OCT, and retinal nerve fiber layer photography, Ophthalmology 114:210, 2007.